Microsc. Microanal. Microstruct. **6** (1995) 127–139 FEBRUARY **1995**, PAGE 127

Classification
Physics Abstracts
07.80 — 78.70D

An EELS and XAS Study of Cubic Boron Nitride Synthesized under High Pressure - High Temperature Conditions

Michel Jaouen([1]), Gilles Hug([2]), Valérie Gonnet([3]), Gérard Demazeau([3]) and Gérard Tourillon([4])

([1])Laboratoire de Métallurgie Physique, URA 131 du CNRS, 40 avenue du Recteur Pineau, 86022 Poitiers Cedex, France
([2])Laboratoire d'Etudes des Microstructures, CNRS-ONERA, B.P. 72, 92322 Châtillon Cedex, France
([3]) Laboratoire de Chimie du Solide du CNRS, UPR 8661 du CNRS, 351, cours de la Libération, 33405 Talence Cedex, France
([4]) Laboratoire d'Utilisation du Rayonnement Electromagnétique, CNRS, CEA, MEN, Centre Universitaire de Paris Sud, Bât. 209D, 91405 Orsay Cedex, France

(Received September 1; accepted December 19, 1994)

Abstract. — Cubic Boron Nitride (c-BN) single-crystals have been synthesized under high pressure and high temperature conditions (HP - HT) using hexagonal Boron Nitride (h-BN) precursors. We have performed a study of both phases with electron (EELS) and X-ray (XAS) spectroscopy that are compared. The c-BN ELNES spectra at B-K and N-K edges are found to be consistent with the XANES (XAS) data, although the energy resolution achieved with X-rays is better than that obtained by EELS with a LaB_6 filament. However, XAS is at a disadvantage by comparison with EELS owing to the presence of the N-K edge second order. Attempts were made to dope c-BN with carbon atoms. The examination of the EELS spectra reveals that the incorporation of carbon species in the BN material is always accompanied by the addition of oxygen. Several samples were analyzed both with selected area electron diffraction and energy loss spectroscopy. Most probed crystals containing C (and therefore O) were found to be hexagonal. These results emphasized that the range of existence of the cubic phase is very narrow around the binary composition.

1. Introduction

Cubic Boron Nitride (c-BN) has exceptional properties and is therefore, as diamond, a very interesting material considering its potential applications [1]. If we compare c-BN and diamond, boron nitride presents some advantages that are:

- high thermal stability,
- lower chemical reactivity with ferrous metals and alloys,

- ability to be n or p doped (for diamond only p-doping is controlled),
- the emission of blue light at the p/n junction opening new developments in optoelectronics.

Compared to diamond, BN is very difficult to synthesize in the cubic phase because it is a binary compound. Many studies have been carried out to obtain c-BN by several deposition methods [2 and Refs. therein]. In most cases, one yields a mixture of phases [3]: cubic, hexagonal (h-BN), turbostratic (t-BN) or amorphous (a-BN). In such cases, electron energy loss (EELS) or X-ray (XAS) spectroscopy can yield information about the nature of the various phases involved in the material. For such a purpose there is a need for standard spectra that can be used as references for further studies. In this paper spectra related to c-BN and h-BN obtained either with EELS or XAS will be presented and compared.

In the last part of this work, we will focus our attention on the possibility of substituting boron or nitrogen by carbon atoms in c-BN. Indeed, due to the difference of electronic population between boron, carbon and nitrogen [4-5], the chemical bonds B-N are different in c-BN compared to C-C bonds in diamond. EELS appears as a possible technique for investigating this problem.

2. Sample Preparation and Experimental Procedure

Up to now, the best way to obtain good c-BN single crystals has been the high pressure - high temperature (HP - HT) technique. The c-BN samples were prepared from a flux-assisted conversion of h-BN used as precursor. The flux precursor was $Ca_3B_3N_4$ with LiF [6]. The pressure and temperature ranges are $5 \leq P \leq 7$ GPa and $1200 \leq T \leq 1400$ °C respectively. For the sample without carbon doping only h-BN is used. The c-BN and non- transformed remaining h-BN crystals are separated from the products issued from the flux precursor or from its decomposition by a washing in heated hydrochloric acid that dissolves these residues. The two phases are then separated by floating in a medium which density is intermediate between those of c-BN (4.450 g/cm^3) and h-BN (2.271 g/cm^3). The resulting c- BN microcrystallites (mean size: 1 mm × 1 mm × 1 mm) were yellow. This results from an excess of nitrogen and a standard EELS quantitative analysis [7] gives $B_{49}N_{51}$ as composition. Concerning the sample with carbon doping, the same flux precursor is used, but 1% (at.) carbon is initially added to h-BN.

For TEM/EELS data acquisition, c-BN and h-BN crystals were mechanically cleaved. The thin flakes are then caught on a 3 mm grid mesh for examination in the microscope. The EELS spectra were acquired on a JEOL 4000FX TEM equipped with a single crystal LaB_6 electron source and fitted with a Gatan model 666 parallel detection electron spectrometer. Spectra recorded in diffraction mode at 400 keV beam energy were corrected for the dark current and channel-to-channel gain variation of the detector. The low-loss and core-loss spectra were collected under the same experimental conditions and from the same region for deconvolution of plural scattering [8]. The energy resolution of the coupled microscope/spectrometer system was determined from a measurement of the full width at half maximum (FWHM) of the spectrum recorded without sample. This was about 1.4 eV.

For XAS measurements, the c-BN crystals were carefully glued on a 3 mm in diameter copper plate. Commercial (De Beers Company, composition: $B_{51}N_{49}$) black c-BN microcrystals were also probed to analyze modifications of the near-edge fine structure (XANES) resulting from compositional changes. The XAS experiments were conducted at the Laboratoire pour l'Utilisation du Rayonnement Electromagnétique (LURE, Orsay, France) on the VUV Super-ACO storage ring. They were carried out on the SACEMOR beam line [9] using a TGM monochromator (B-K edge: 1800 lines/mm grating, N-K edge: 800 lines/mm grating). The energy resolution at the C-K edge is better than 80 meV. For XAS the incident beam I_0 was monitored by collecting the total yield

from a 85% transmission copper grid freshly coated with gold. The total electron yield from the sample I was then normalized with respect to I_0. The electrons were collected over 1s for each data point, the energy step being 0.1 eV.

3. EELS and XAS c-BN and h-BN Spectra

3.1 TEM AND EELS RESULTS. — The very good quality of the c-BN crystals obtained by the HP-HT method is confirmed by the electron diffraction pattern shown in the inset of Figure 1. One only observes intense spots that correspond to the (100) plane of c-BN. We deduce a lattice parameter equal to 3.61 ± 0.01 Å, a value very close to that reported [10] in the literature (3.615 ± 0.001 Å). The bright field image (Fig. 1) shows that the c-BN sample is free from defects, only cleavage steps are visible. The low-loss spectra related to c-BN and h-BN are plotted in Figure 2. They show plasmon energies of 30.4 and 25.3 eV respectively, values that are 1.4 eV higher than those quoted in reference 3. One should observe the existence of a π^* plasmon characteristic of the hexagonal structure [11] at about 8 eV for the h-BN sample. The plasmon energy provides a useful measure of the density of BN samples (3.450 g/cm^3 for c-BN, 2.271 g/cm^3 for h-BN) assuming the number of nearly free electrons is on average four per atom, whatever the bonding arrangement is. In this case the squared ratio of the plasmon energies c-BN over h- BN must be equal to the ratio of densities. Obviously this assumption is not fulfilled since we obtain 1.44 instead of 1.519. The most probable explanation of such a behavior may result from the existence of different effective electron masses in c-BN and h-BN materials. Finally, it must be pointed out that the c-BN and diamond plasmon shapes look very similar [12]. In particular, both exhibit a hump towards the low energy side of the σ^* plasmon (around 23 eV for c-BN) that can be attributed to surface plasmons [8].

In Figures 3 and 4 are shown the c-BN and h-BN ELNES spectra related to B-K and N-K edges respectively. They were recorded with an energy dispersion of 0.1 eV per channel and a small collection angle ($2\beta = 2$ mrad). For each spectrum, 10 read-outs were used with 2 seconds of integration time per read-out. The B-K and N-K edges of hexagonal boron nitride, like the C-K edge of graphite [13], show separate peaks due to transitions of the 1 s electrons to π^* empty antibonding orbitals and σ^* bands. Their intensities strongly depend on the orientation of the

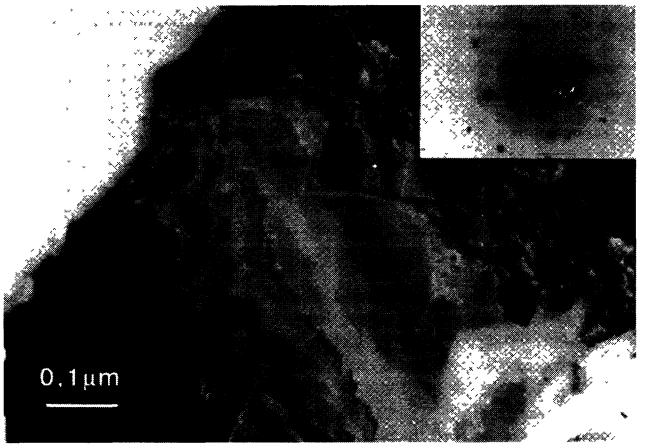

Fig. 1. — c-BN bright field image. Inset: diffraction pattern indexable as (100) plane.

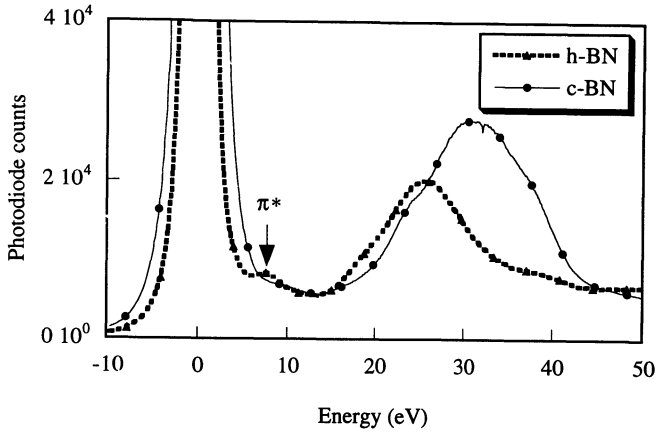

Fig. 2. — c-BN (full line, circles) and h-BN (dotted line, triangles) low-loss spectra.

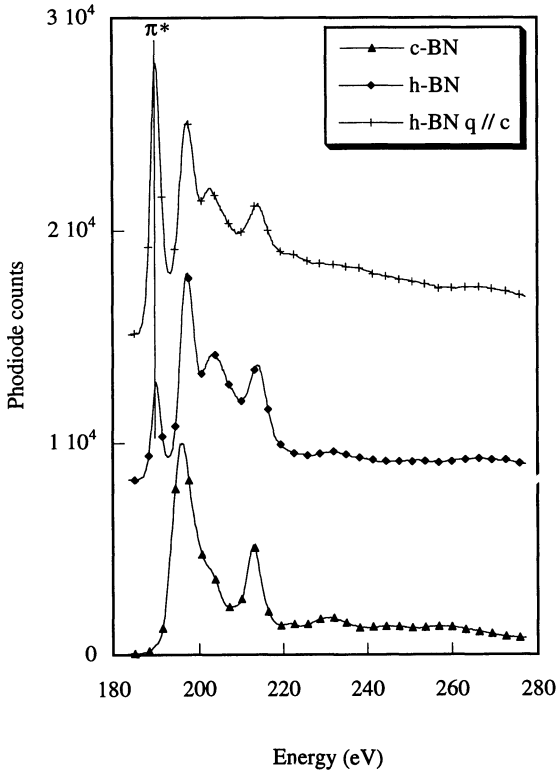

Fig. 3. — ELNES B-K edge spectra of c-BN (triangles) and h-BN (lozenges: random orientation, crosses: $q//c$) samples.

sample c-axis with respect to the incident electron beam [14]. Indeed if one uses small apertures, the distribution of π^* scattering is forward-peaked when the scattering vector **q** is parallel to the c-axis and therefore the π^* resonance enhanced. On the opposite, **q** has no component in the direction of the π-bonding when the incident electron beam is parallel to the cleavage plane and

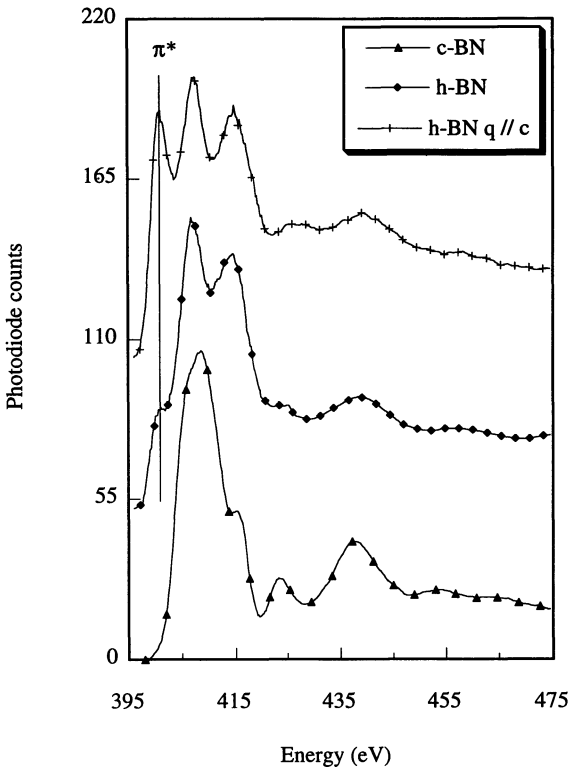

Fig. 4. — ELNES N-K edge spectra of c-BN (triangles) and h-BN (lozenges: random orientation, crosses: $q//c$) samples.

the π^* resonance drop to zero [8]. This behavior can be observed at both B-K and N-K edges but unfortunately we have not been able to find a single h-BN crystal that can be tilted over 90 to verify entirely this point. It must also be pointed out that the π^* resonance intensity at the B-K edge is much higher than that observed at the N-K edge. This occurs because the densities of empty π^* states are different for boron and nitrogen atoms owing to their distinct valence states [4]. All these features are characteristic of sp^2 hybridized materials. In return, for sp^3 hydridization, we do not observe such π^* resonances. Thus, the presence or not of π^* structures can be used as a fingerprint to assess the nature of the phase of boron nitride samples.

3.2 XAS RESULTS. — The spectra related to B-K and N-K h-BN are displayed in Figures 5 and 6 respectively. However, compared to EELS, the polarization effects are stronger due partially to a better energy resolution, but this is not the only reason. Indeed, a comparison [15] of high energy resolution EELS and XAS experiments performed at the diamond C-K edge show a similar reduction of the exciton line magnitude in EELS with respect to the XAS results. It has been suggested [15] that there exists close to the edge in EELS some core hole screening effect induced by the primary swift electron that remains present near the core hole for a significant part of the time it takes for the core electron to make the transition from the core level to the exciton orbital. Using the same idea, one may suggest that the π^* orbital is grossly elongated in the direction anti-parallel to the swift electron trajectory so that the overlap between the initial and final wavefunctions decreases, resulting in a reduction of the π^* resonance intensity in EELS compared to

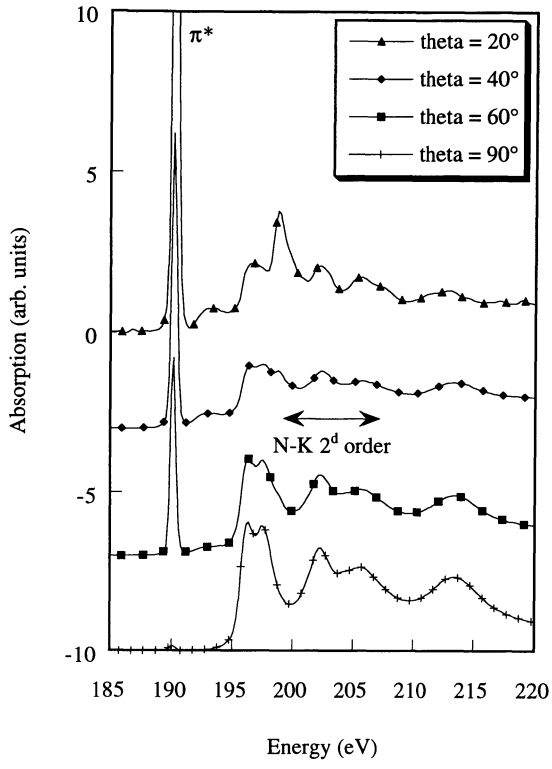

Fig. 5. — XANES B-K edge spectra of h-BN showing the N-K edge second order contribution. Theta is the angle between the incident wave electric field **E** and the *c*-axis.

that observed in XAS, where no such effect occurs.

From an experimental point of view, it is quite easy to study polarization effects in XAS because one has only to rotate the sample with respect to the incident photon beam (the electric field **E** of the incoming electromagnetic wave plays the role of the scattering vector **q**). We can note on the B-K edge spectra the presence (around 200 eV) of structures that are not observed by EELS (Fig. 3). These additional structures are due to the grating second order and they correspond to the N-K edge spectra at half energy that superimpose on the B-K ones. The existence of these higher order spectra is inevitable whenever gratings are used to monochromatize soft X-rays. This complicates strongly the analysis as it is shown in Figure 7 where the B-K XANES spectra are plotted for two c-BN compositions. However, one can obtain some useful information from these data.

The sample A, elaborated with the HP-HT method, is obviously composed of a mixture of phases owing to the presence of a visible π^* resonance. This implies that not all h- BN precursors have been transformed into c-BN during the HP-HT process. This point was confirmed by FTIR spectroscopy, which shows a weak contribution from the hexagonal phase to the spectrum. In XAS, the surface of the sample irradiated by the X-rays is about 1 mm^2 and then several crystallites are simultaneously illuminated. Therefore, if some of them belong to the hexagonal phase, they will contribute to the measured current. The result is that the A sample XANES spectrum can be considered as an addition of c-BN and h-BN spectra. We did not try to make a linear combination of c-BN and h-BN data to fit this XANES spectrum owing to the too-strong h-BN orientation

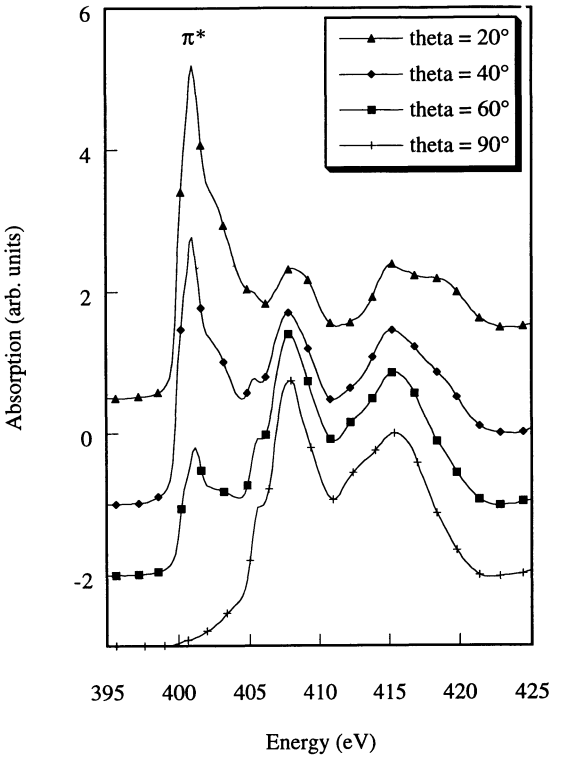

Fig. 6. — XANES N-K edge spectra of h-BN. Theta is the angle between the incident wave electric field **E** and the *c*-axis.

dependence mentioned above. However, the c-BN component must be very small because the π^* resonance is very weak and narrow.

The sample B (De Beers) is purely cubic. We do not observe any visible π^* structure, but only a small hump at the beginning of the edge jump that is predicted by pseudo-atomic- orbital calculations [16]. We also recognize the N-K edge second order that is much more important here than for sample A. We do not have an explanation that will justify such a difference. In the same way, it remains to elucidate the great difference of amplitude observed between EELS and XAS data on the first peak at the onset of the c-BN B-K edge. This may come from the difference between electron and X-rays cross-sections, but this assumption needs further study.

The comparison of the c-BN N-K edge EELS and XAS data is much more favorable as it is shown in Figure 8. Here, both techniques give similar results, except that the energy resolution is better for XAS than that obtained from EELS with a LaB_6 electron source. This good energy resolution makes XAS very sensitive to small changes of composition: a variation of 4% of the boron content (A: $B_{49}N_{51}$, B: $B_{51}N_{49}$) appears as an inversion of the amplitude of the two small peaks localized at the top of the edge jump, the same behavior being also visible on the N-K second order (Fig. 7)! One can note the small humps at the foot of the N-K edge jump in XANES spectra (arrow in Fig. 8). They may be due to band structure effects, as predicted by theoretical calculations [16]; but for sample A, a small π^* contribution cannot be excluded.

To end this section, we discuss the advantages and disadvantages of both techniques, and their complementarity. One of the main advantages of EELS over XAS is its great selectivity, the

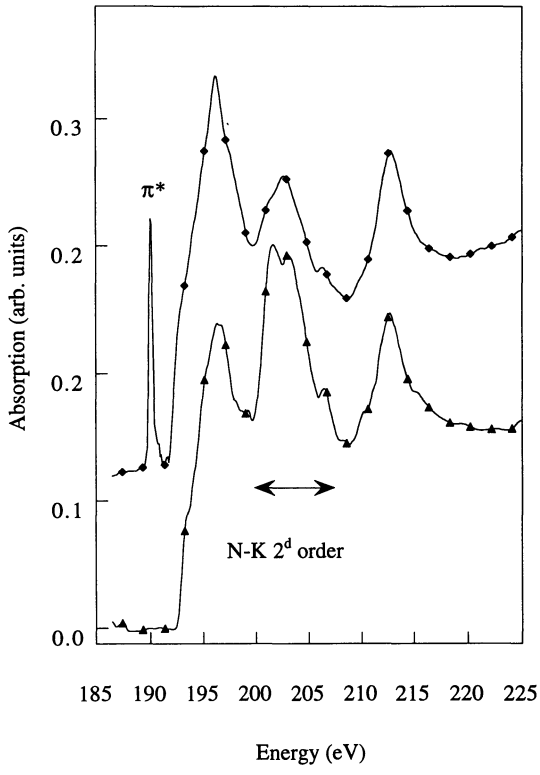

Fig. 7. — XANES B-K edge of c-BN. Lozenges : sample A ($B_{49}N_{51}$, HP-HT). Triangles : sample B ($B_{51}N_{49}$, De Beers Compagny).

probed volume being much smaller [17]. Therefore EELS allows one to analyze multiphase materials, a point of great importance for numerous studies. For example it is easier, using the momentum-selection possibility for ELNES, to study polarization effects that can be difficult to analyze in XAS as soon as the probed area is either polycrystalline or multiphased (see the XANES data related to sample A in Fig. 7). When combined with TEM, one also obtains the use of all the analytical tools of the microscope: electron selected area diffraction and imaging. However this requires one to thin the sample and some mathematical manipulations of the data (plural scattering deconvolution, background removal) that must be done with care. In return, XAS offers better energy resolution than EELS, at least when a LaB_6 electron source is used, and the spectra are immediately interpretable. Furthermore the energy scale in XAS is absolute. For instance, one can use the carbon contamination of the optics to calibrate the monochromator. This allows one to study very small shifts induced by chemical effects on the edge energy, something not as easy to perform with a parallel detection electron spectrometer. Finally, it should be remembered that VUV XAS in the total electron yield mode is very surface sensitive, the estimated probed depths varying in the range 5 – 8 nm [18]. One can then study how the free surface of the sample is terminated, how it traps the contaminants, their nature; all these questions being of a great significance when one wants to use c-BN in electronic devices.

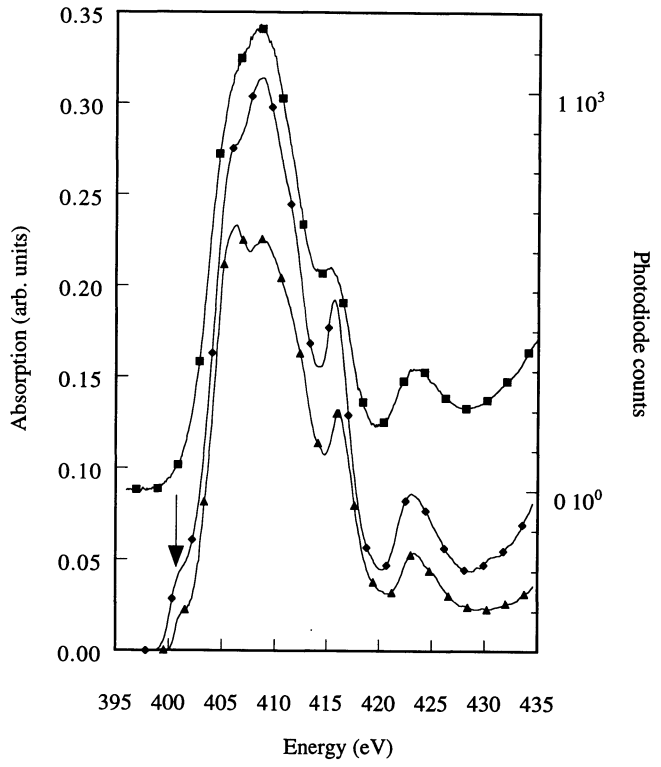

Fig. 8. — Top: $B_{49}N_{51}$ N-K edge ELNES (squares). Middle: $B_{49}N_{51}$ N-K edge XANES (lozenges) Bottom: $B_{51}N_{49}$ N-K edge XANES (triangles).

4. EELS Study of BN Doped with Carbon

Diamond and c-BN have the same structure (zincblende, space group $F\bar{4}3m$) and therefore it is interesting to know if it is possible to substitute boron or nitrogen with carbon atoms. The main point of interest with this kind of study is that it could provide some information about the range of existence of the cubic phase. EELS can help answer the two following questions. First, do the carbon atoms participate to the cubic network? Second, what are the sites of substitution: boron or nitrogen?

Using the synthesis conditions described in section 2, we performed some TEM (SAD, imaging) and EELS preliminary experiments. At first, we never detect amorphous BN. In some cases, we find areas that correspond to a material that is either purely cubic or purely hexagonal. These areas are not of interest for the present purpose, however this means that the incorporation of carbon in the BN matrix is not a homogeneous process. In return, each time we detect the presence of carbon, the related electron selected area diffraction pattern is indexable as h-BN. The associated bright field images show that the crystals then contain many defects (stacking faults, dislocations) as illustrated in Figure 9. Furthermore, the examination of the EELS spectra reveals that the incorporation of carbon in the BN material is always accompanied by the addition of oxygen. A typical example of the corresponding EELS data is shown in Figure 10 (these data were acquired with an energy dispersion of 1 eV, 10 read-outs, integration time for each of them: 2 seconds). In this particular case, a crude quantitative analysis gives as composition $B_{44}N_{45}C_6O_5$. One easily

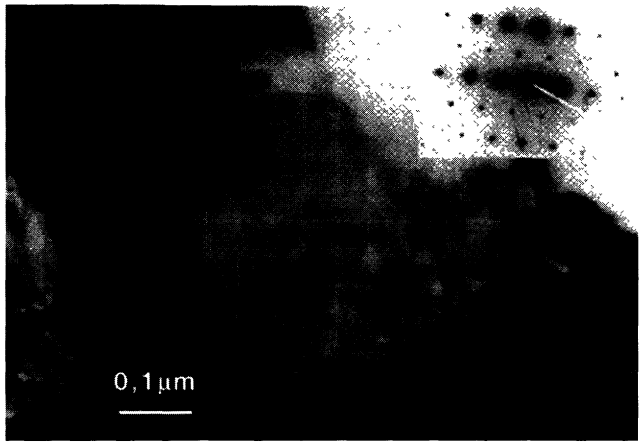

Fig. 9. — BN_{1-x} C_x bright field image. Inset: diffraction pattern indexable as $(0\bar{1}11)$ plane.

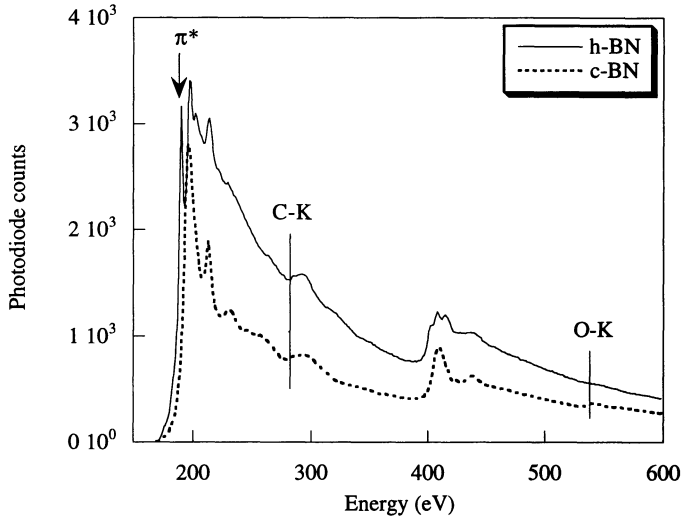

Fig. 10. — EELS spectra of carbon doped BN showing C-K and O-K edges for hexagonal (full line) and cubic (dotted line) areas.

recognize on this spectrum the characteristic features of the hexagonal structure. In Figure 11 is plotted an enlarge view of the C-K, N-K and O-K edges. We see in the C-K edge a hump that may correspond to a π^* resonance characteristic of sp^2 hybridized carbon atoms. It also shows marked EXELFS oscillations up to the N-K edge that are quite different from those observed in amorphous carbon [11]. These well-defined EXELFS oscillations correspond to the existence of long- range order around the carbon atoms since they result in an interference process between the outgoing electron wave and the wavelets back-scattered by each neighbour of the central excited atom. For the area analysed here, we conclude that some carbon atoms, if not all, belong to the crystal network.

This behavior is general for the approximately ten areas that we have analyzed, except for one

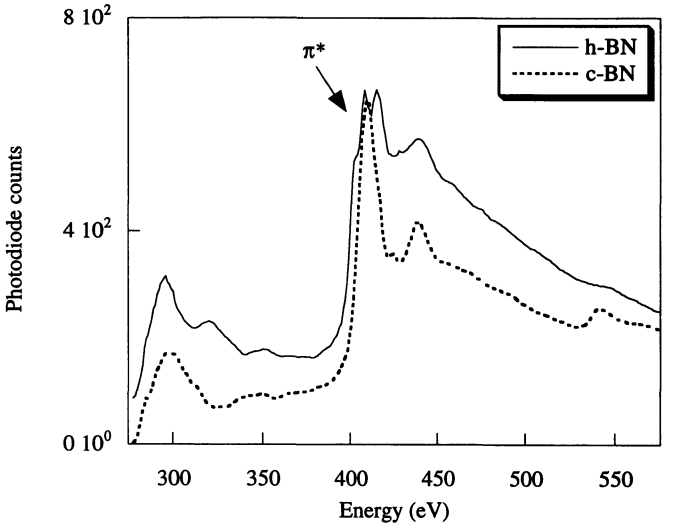

Fig. 11. — C-K to O-K edges enlarged view of Figure 11.

of them. The related EELS spectrum is shown in Figure 10. The shapes of the B-K and N-K edges are unambiguously those observed for a truly cubic material (cf. Figs. 3 and 4). This was confirmed by selected area electron diffraction. We have not been able to perform a quantitative analysis in this case due to the strong boron EXELFS oscillations that forbid any reliable C-K edge background removal. This point explains the rather distorted base line on the enlarged view of the C-K to O-K edges plotted in Figure 11. Here, as for amorphous carbon materials, one observes only one oscillation after the broad σ^* band at the onset of the C-K edge. It corresponds to carbon atoms that do not fit in the c-BN lattice. They more probably precipitate at the grain boundaries or as subnanometer clusters. This assumption needs to be confirmed with more detailed TEM observations. Nevertheless, from all the results quoted in the present paper, it seems that the range of existence of the cubic phase is very narrow around the equiatomic composition.

It remains to explain the unexpected presence of oxygen (that seems to be particularly important for the area described above). We do not believe that it comes from contamination of the microscope column because we do not observe its presence (nor that of carbon) on the c-BN and h-BN references. We presume that the oxygen comes from the particular synthesis conditions ($P = 6.5$ GPa, $T = 1400$ °C) that have been used in the present case. Without carbon incorporation into the HP-HT cell, they lead to the formation of perfect c-BN crystals like the one shown in Figure 1. This result suggests that the range of pressure-temperature needed to obtain a zincblende $BN_{1-x}C_x (x \approx 1\%)$ is displaced towards higher values than those required to obtain c-BN without carbon. Indeed, a very recent work [19] shows that one can obtain a zincblende phase from the precursor $BN_{1-x}C_x$ using shock-waves method. In this mode of compression, the pressure can be as high as 60 GPa. Unfortunately, no characterisation at the carbon site has been performed. Thus, it is not surprising that a pressure of 6.5 GPa yields an inhomogeneous transformation and therefore heterogeneous crystals that are easily oxidized during the chemical treatment described in section 2. Consequently, the oxygen is not incorporated in the material during the reaction between the h-BN precursors and carbon into the HP-HT cell. Thus, the presence of oxygen does not obviate the difficulty we have found in synthesizing the cubic $BN_{1-x}C_x$ phase using our P-T conditions. Therefore, for the study of interest, we must employ a pressure higher than the one we have used to synthesise cubic $BN_{1-x}C_x$ crystals.

Our results, compared to those reported in reference [19], suggest that the solid solution c-BN - diamond is an out-of-equilibrium phase that may be obtained only under particular P-T conditions like the compression induced by shock-waves. Such behaviour may come from the difference of the chemical bonds between $B(2s^2\ 2p^1)$ and $N(2s^2\ 2p^3)$ into the c-BN network where the sp^3 hybridisation leads to an empty sp^3 orbital on the boron site and to one filled and three half-filled sp^3 orbitals on the nitrogen site; the carbon being characterised by four half-filled sp^3 orbitals. Furthermore, a clear answer to the two questions given previously requires more sophisticated tools. In particular, it will be very interesting to perform EELS imaging (EELSI) in a high energy resolution STEM that could allow us to determinate at the atomic scale [20] the localisation of the carbon in the c-BN matrix.

5. Conclusion

In this paper, we have presented EELS and XAS spectra obtained on h-BN and c-BN materials. We have shown that the c-BN samples elaborated with a HP-HT method are of very good quality. The related EELS data can be considered as references for data base. We have discussed the advantages and disadvantages of EELS regarding XAS, as well as their complementarity. EELS offers good spatial resolution whereas XAS, which is more surface sensitive, presents higher energy resolution. We have also undertaken preliminary experiments to assess the possibility of carbon doping a c-BN material. We have shown that we did not presently succeed to obtain carbon doped c-BN, probably because we have used a too-low pressure during the HP-HT synthesis process. We also suggest that EELSI will be a better adapted technique to study this problem.

References

[1] Vel L., Demazeau G. and Etourneau J., *Mater. Sci. Eng., Solid State Mater. Ad. Technol.* **B10** (1991) 149.

[2] Tanabe N. and Iwaki M., *Nucl. Instr. Meth.* **B80/81** (1993) 1349.

[3] McKenzie D.R., Cockayne D.J.H., Muller D.A., Murakawa M., Miyake S., Watanabe S. and Fallon P., *J. Appl. Phys.* **70** (1991) 3007.

[4] Xu Y.N. and Ching W.Y., *Phys. Rev.* **B44** (1991) 7787.

[5] Matar S., Gonnet V. and Demazeau G., *J. Phys. I France* **4** (1994) 335.

[6] Vel L. and Demazeau G., *Solid State Comm.* **79** (1991) 1.

[7] Leapman R.D. in: Transmission Electron Energy Loss Spectometry in Materials Science, M.M. Disko, C.C. Ahn and B. Fultz Eds. (EMPMD Monograph Series 1992) p. 47.

[8] Egerton R.F., in: Electron Energy Loss Spectroscopy in the Electron Microscope (Plenum Press, New York and London 1989).

[9] P. Parent, C. Laffon, A. Cassuto and G. Tourillon, *J. Phys. Chem.*, in press.

[10] Wentorf Jr. R.H., *J. Chem. Phys.* **26** (1957) 956.

[11] Bhushan B., Kellock A.J., Cho N. and Ager III J.W., *J. Mater. Res.* **7** (1992) 404.

[12] Bozzolo N., Hug G., Jaouen M. and Bauer-Grosse E., ICEM 13 Paris, Les Editions de Physique **2A** (1994) 577.

[13] Egerton R.F. and Whelan M.J., *J. Electron. Spectrosc.* **3** (1974) 232

[14] Leapman R.D., Fejes P.L. and Silcox J., *Phys. Rev.* **B28** (1983) 2361.

[15] Batson P.E. and Bruley J., *Phys. Rev. Lett.* **67** (1991) 350. Batson P.E., in: Transmission Electron Energy Loss Spectometry in Materials Science, M.M. Disko, C.C. Ahn and B. Fultz Eds. (EMPMD Monograph Series 1992) p. 217.

[16] Rez P., Weng X. and Ma H., *Micros. Microanal. Microstruct.* **2** (1991) 143.

[17] Blanche G., Hug G., Jaouen M. and Flank A.M., *Ultramic.* **50** (1993) 141.

[18] Stöhr J., in: NEXAFS Spectroscopy (Spinger-Verlag New York Berlin Heidelberg 1992).

[19] Kakudate Y., Yokoi H., Yoshida M., Usuba S., Fujiwara S., Kawaguchi M., Kawashima T. andKomatsu T., 4th International Conference on the New Diamond Science and Technology, KOBE (July 18-22th 1994), Program-Abstracts 105 (Proceedings in press).

[20] Brown L.M., *Nature* **366** (1993) 721. Muller D.A., Tzou Y., Raj R. and Silcox J., *Nature* **366** (1993) 725; Batson P.E., *Nature* **366** (1993) 727.